

**FIRBACK FAR INFRARED SURVEY WITH ISO:
DATA REDUCTION, ANALYSIS AND FIRST RESULTS**

H. Dole¹, G. Lagache¹, J-L. Puget¹, R. Gispert¹, H. Aussel^{2,7}, F.R. Bouchet³,
C. Ciliegi⁴, D.L. Clements⁵, C.J. Cesarsky², F.-X. Désert⁶, D. Elbaz², A. Franceschini⁷,
B. Guiderdoni³, M. Harwit⁸, R. Laureijs⁹, D. Lemke¹⁰, R. McMahon¹¹, A.F.M. Moorwood¹²,
S. Oliver¹³, W.T. Reach¹⁴, M. Rowan-Robinson¹³, M. Stichel¹⁰

¹Institut d'Astrophysique Spatiale, Orsay, France

²Service d'Astrophysique, CEA/DSM/DAPNIA Saclay, France

³Institut d'Astrophysique de Paris, France

⁴Osservatorio Astronomico di Bologna, Italy

⁵Cardiff University, UK

⁶Laboratoire d'Astrophysique, Observatoire de Grenoble, France

⁷Osservatorio Astronomico di Padova, Italy

⁸511 H.Street S.W., Washington, DC 20024-2725

⁹ISOC ESA, VILSPA, Madrid, Spain

¹⁰MPIA, Heidelberg, Germany

¹¹Institute for Astronomy, University of Cambridge, UK

¹²ESO, Garching, Germany

¹³Imperial College, London, UK

¹⁴IPAC, Pasadena, CA, USA

ABSTRACT

FIRBACK is one of the deepest cosmological surveys performed in the far infrared, using ISOPHOT. We describe this survey, its data reduction and analysis. We present the maps of fields at $175 \mu\text{m}$. We point out some first results: source identifications with radio and mid infrared, and source counts at $175 \mu\text{m}$. These two results suggest that half of the FIRBACK sources are probably at redshifts greater than 1. We also present briefly the large follow-up program.

Key words: ISOPHOT; far infrared survey; cosmology; galaxy evolution

1. INTRODUCTION

The discovery of the Cosmic Far Infrared Background Radiation (CFIBR) (Puget et al. 1996, Fixsen et al. 1998, Hauser et al. 1998, Lagache et al. 1999) using COBE data and constraints on its spectrum, demonstrates that about two thirds of the light emitted by galaxies integrated over all redshifts has been processed by dust and released at FIR and submm wavelengths. This background is in line with models using strong evolution of galaxies.

Studying the population of galaxies radiating mostly at long wavelengths as a function of redshift is thus one of the important but difficult observational tasks

of today in the field of galaxy formation and evolution (see Puget & Lagache, these proceedings).

In this context, FIRBACK, which is a cosmological survey dedicated to a study of the Cosmic Far Infrared Background and galaxies contributing to it, is one important step.

2. DATA SET

FIRBACK is a survey of 3 main fields (described in Table 1) covering 4 square degrees using ISOPHOT. All fields have been observed in raster mode (AOT P22) with the C200 detector and C_160 filter centered at $\lambda = 175 \mu\text{m}$. We have also additional ISO observations with ISOPHOT and ISOCAM (see below).

Table 1. Fields of the FIRBACK survey.

Field Name	α_{2000}	δ_{2000}	l	b	area
	h min	deg min	deg	deg	sq deg
Marano	03 11	-54 45	270	-52	1
ELAIS N1	16 11	+54 25	84	+45	2
ELAIS N2	16 36	+41 05	65	+42	1

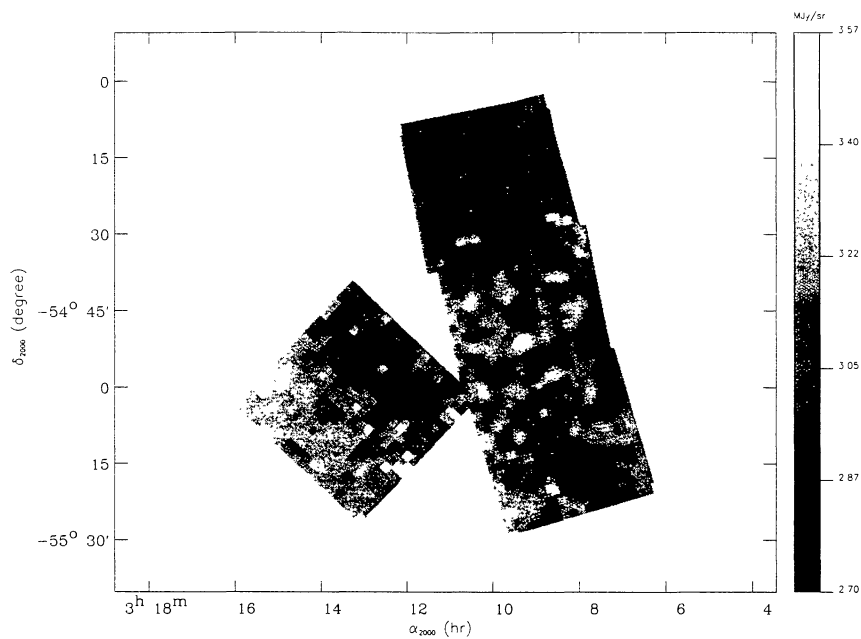


Figure 1. Map of FIRBACK Marano fields

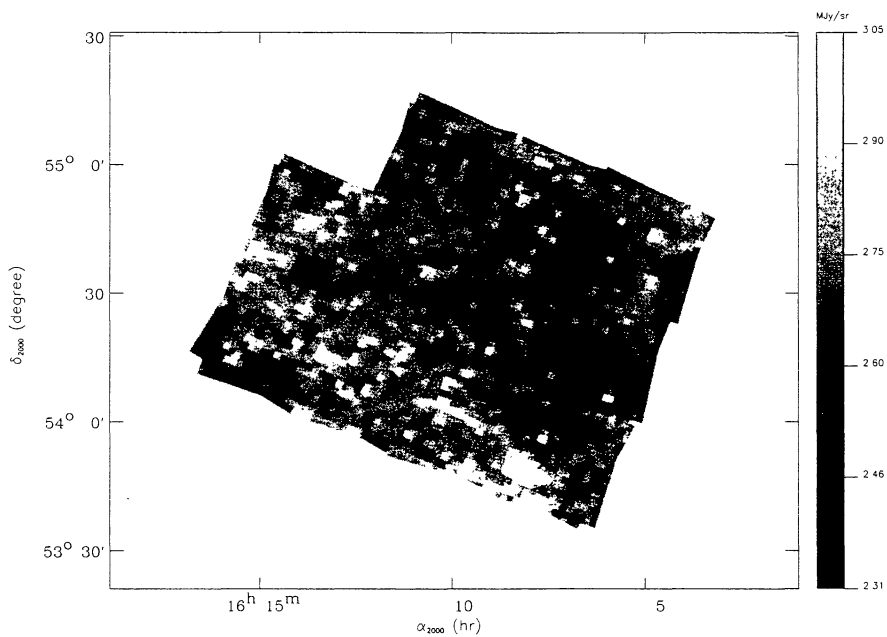


Figure 2. Map of FIRBACK ELAIS N1 field

FIRBACK Marano

This area (map Figure 1) is composed of four individual fields, called Marano 1, 2, 3 and 4, which have been observed four times. The redundancy goes from 32 (in overlapping regions) to 1 (on the edges) with an average of 16, and the oversampling is optimal in both Y and Z directions in Marano 2, 3 and 4

(half pixel offset between rasters). Marano 1 covers $31.5' \times 31.5'$, and Marano 2, 3 and 4 about $77' \times 26'$. Integration time per sky pixel is 256 s on average. *Additional observations:* in Marano 1 we have one P25 absolute measurement, five small rasters at $90 \mu\text{m}$ (not yet reduced); in the complete Marano field, we have a $15 \mu\text{m}$ ISOCAM survey.

FIRBACK ELAIS N1

This area (map Figure 2) is composed of eleven individual fields, observed 2 times with an offset of less than a pixel, and the redundancy goes from 16 (in overlapping regions) to 1 (on the edges) with an average of 8. ELAIS N1 covers about 2 square degrees. Integration time per sky pixel is 128 s on average. Note that the northern FIRBACK fields have been chosen to cover some corresponding ELAIS fields at other wavelengths (see Rowan-Robinson et al., these proceedings).

FIRBACK ELAIS N2

This area (map Figure 3) is composed of nine individual fields, observed 2 times with an offset of one pixel, so the redundancy is 8 on average, without oversampling. ELAIS N2 covers about $57' \times 57'$.

3. DATA REDUCTION

3.1. From raw data to AAP

We used PIA¹ version 7.2.2 (PHT Interactive Analysis, Gabriel et al. 1997) to reduce data from ERD (Edited Raw Data, the lowest level) to AAP (Auto Analysis Product Data, level where flux density and positions are available):

- ERD to SRD (Signal per Ramp Data): linearisation, deglitching, fit ramps to first order
- SRD to SCP (Signal per Chopper Plateau Data): deglitching, no drift correction
- SCP to AAP: no reset interval correction (reset times are identical), subtraction of dark current, power calibration using interpolation between 2 FCS. We then used our own IDL routines to correct for transients induced by strong glitches, and to perform a flat correction using observational redundancies.

¹PIA is a joint development by the ESA Astrophysics Division and the ISOPHOT Consortium

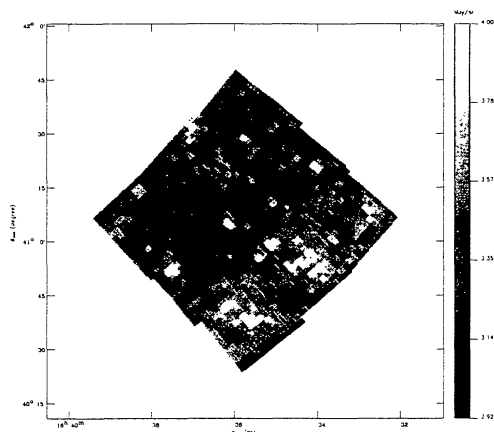


Figure 3. Map of FIRBACK ELAIS N2 field

3.2. Map projection

Our basic data projection is performed in two steps: (1) geometrical grid computation and (2) projection of the signal.

- The first step is the most time consuming. We read all AAP data of one complete field, and create a large grid in (α, δ) with tunable pixel sizes (usually 10 arc-sec); this step has to be performed just one time.
- The second step just acts to restore the grid, to coadd individual raster data onto the grid by distributing the pixel signal in the area of one pixel, and by updating a weighting map.

This method is well-suited to large amounts of data, in terms of sky surface or number of co-added rasters with different roll angles. Figures 1, 2 and 3 show such maps.

4. RESULTS

4.1. Source detection

Source detection is directly performed on final co-added maps, using eye recognition to discriminate point sources from cirrus structure. We then computed the flux by aperture photometry with radii chosen to minimize noise in source detection $R_{min} = 60''$ and $R_{max} = 92''$ (Puget et al. 1999).

4.2. Catalogs and identifications

Sources in our catalog have a S/N ratio greater than 3, and photometric accuracy is about 30 %. Fluxes are in the range 75 mJy to 1.6 Jy, with an average of 252 mJy and a median of 175 mJy.

In order to constrain both Spectral Energy Distribution (SED) and position of these sources, we looked for identifications: Table 2 gives a summary of detected sources and identifications with ISO or ground-based radio telescopes.

In the *Marano Field*, we performed a smaller $15 \mu\text{m}$ survey using ISOCAM (Désert et al. 1998), which covers about 50 % of the $175 \mu\text{m}$ survey surface. Radio identifications are performed using Australia Telescope Compact Array available data (Grupponi et al. 1997) or preliminary data of our program being reduced, that is why 8 identifications is a lower limit. The situation is different in northern fields *ELAIS N1 & N2* because the ELAIS consortium performed observations using ISO at $\lambda = 15 \mu\text{m}$, $\lambda = 90 \mu\text{m}$ (Rowan-Robinson et al., these proceedings), using the VLA at $\lambda = 20 \text{ cm}$ (Ciliegi et al. 1998), and at other wavelengths. Most of the 31 sources with $90 \mu\text{m}$ counterpart have a color ratio $\frac{F_{175 \mu\text{m}}}{F_{90 \mu\text{m}} \text{ PHOT}} \geq 2$, which has to be compared to local sources ($z \leq 0.1$) where $\frac{F_{175 \mu\text{m}}}{F_{100 \mu\text{m}} \text{ IRAS}} \simeq 1$ (Stickel et al. 1998), suggesting that a significant proportion of FIRBACK sources are large-redshift sources (see discussion below). Most of NED² identifications are FIRST (Becker et al. 1995) or IRAS sources.

²The NASA/IPAC Extragalactic Database (NED) is operated by the Jet Propulsion Laboratory, California Institute of Technology, under contract with the National Aeronautics and Space Administration

Table 2. Number of FIRBACK sources and identifications

Field Name	175 μm	15 μm	90 μm	20 cm
F_ν (mJy) \geq	75	1	60	0.2
Marano	78	29	no data	≥ 8
ELAIS N1	113	19	18	20
ELAIS N2	85	no data	13	22

4.3. Source counts

We present raw source counts in Figure 4, using sources coming from FIRBACK ELAIS N1, N2 and Marano 2 3 4 fields (208 sources brighter than 100 mJy in less than 3 square degrees). Raw counts means here that *counts are not corrected for incompleteness*. For $\log(S \geq 300 \text{ mJy})$, counts are not expected to change a lot due to incompleteness correction, so the steep slope of 2.20 is a minimum. We also plotted Marano 1 raw counts (Puget et al. 1999) which are higher by a factor 2 but compatible within uncertainties, probably because based on 22 sources in a smaller area (0.25 square degree), Kawara et al. (1998) data in the Lockman Hole (difficult to see in the plot because their count at 150 mJy gives the same number as ours), models with and without evolution from Franceschini et al. (1998), and model E from Guiderdoni et al. (1998). Compared to extrapolated IRAS counts, FIRBACK counts are about 20 times higher at 200 mJy. Our counts are not compatible with non-evolution models and need strong evolution. Model with evolution from Franceschini et al. (1998) predicts smoother slopes than observed, whereas model E from Guiderdoni et al. (1998) fits roughly the slope even if lower than observed.

5. FOLLOW-UP ³

An intensive multiwavelength follow-up program is being performed.

In the *Marano field*, we are following-up at $\lambda = 20$ cm using the Australia Telescope Compact Array in compact configurations (data being reduced) and extended configuration (program to submit)(Dole). In the optical range, one source has been observed with the NTT (Dennefeld).

In the *ELAIS N1 & N2 fields* at millimetre wavelengths, we are following-up using the IRAM 30 m antenna and Plateau de Bure Interferometer (Omont & Guiderdoni). Submillimetre observations in N1 are scheduled at JCMT (Scott) and in April at CSO (Lagache), and optical follow-up of sources is performed at Palomar (Reach).

³extended FIRBACK collaboration for follow-up also includes: D. Benford, P. Cox, M. Dennefeld, G. Helou, R. Mac Mahon, A. Omont, F. Pajot, T. Phillips, D. Scott, F. Viallefond

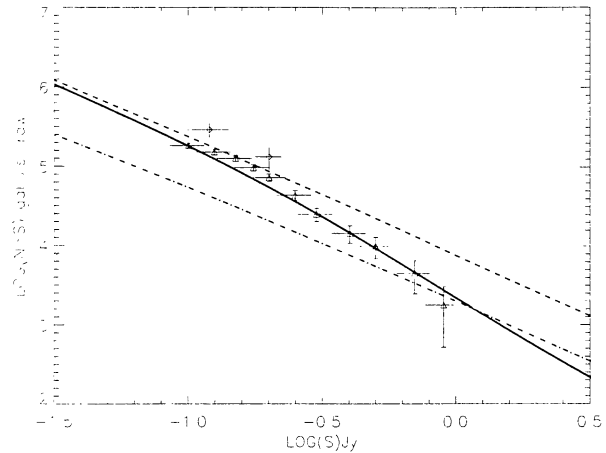


Figure 4. Source counts with FIRBACK data in Marano 1, 2, 3, 4, ELAIS N1 and ELAIS N2. These counts are not corrected for incompleteness. Data: diamonds: Marano 1 (Puget et al. 1999); triangles: ELAIS N1, N2 and Marano 2 3 4; Lockman Hole data (Kawara et al. 1998); purple star at 150 mJy, superimposed on our counts. Models: Guiderdoni et al. 1998: blue line: model E; Franceschini et al. 1998: red dash-dash: with evolution; green dash-dot: without evolution

6. DISCUSSION ON COSMOLOGICAL IMPLICATIONS

6.1. Population

The steep slope of the number counts (≥ 2.2) cannot be accounted for by the effect of the K-correction (ratio, at a given wavelength, of the emitted flux and the observed flux with a spectral redshift) if no cosmological evolution is present as can be seen in Figure 4. The Guiderdoni et al. (1998) model which gives rather a good fit to our counts presents a strong evolution for the star burst component ($\propto (1+z)^5$) and an ULIRG (Ultra Luminous Infrared Galaxies) component. In this model, the far infrared background comoving luminosity per unit volume increases by a factor of 20 from $z = 0$ to $z = 2.5$.

This model also predicts a redshift distribution for sources brighter than 100 mJy at 175 μm . The redshift distribution peaks at $z = 0.9$ with a median of $z = 1.0$, about half of the sources lie at redshift between 1 and 2, and about 10% above $z = 2$. Furthermore, this model is compatible with the far infrared background detected in the COBE data. Sources detected in our survey account for 3% of this background at 175 μm , and the model predicts that 90% of the background is made of sources brighter than 2 mJy; this predicted value is probably too low, because our slope is higher than the model, and our counts are not yet corrected for incompleteness.

6.2. Identifications

If these galaxies are star burst galaxies with a SED peaking at 75 μm , a typical source observed close to

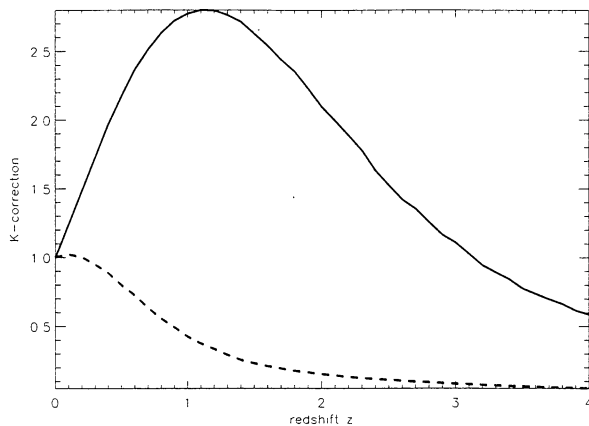


Figure 5. *K*-correction at $175\ \mu\text{m}$ (black line) and $90\ \mu\text{m}$ (blue dash-dash line) as a function of redshift for a starburst galaxy whose SED peaks at $75\ \mu\text{m}$

our detection limit ($F_{175\ \mu\text{m}} = 100\ \text{mJy}$) has a luminosity $1.2 \times 10^{12} L_{\odot}$ (in a $h = 0.5$ and $\Omega_0 = 1$ cosmology).

The same source will have $F_{15\ \mu\text{m}} \simeq 1\ \text{mJy}$ and thus is easily detectable with ISOCAM. One of the differences between mid- and far-infrared observations is that the *K*-correction allows observation of galaxies with redshifts in general below 1.4 (because of the PAH feature's cutoff) in the mid infrared; no such strong limit exists in the far infrared. We have only 25% detections at $15\ \mu\text{m}$, implying that more than half of the sources are at $z > 1.4$ (redshift at which $15\ \mu\text{m}$ flux drops sharply).

The expected $90\ \mu\text{m}$ flux for this source is $F_{90\ \mu\text{m}} \simeq 40\ \text{mJy}$, and thus not easily detectable in the ELAIS survey. Furthermore, the *K*-correction at 90 and $175\ \mu\text{m}$ as function of redshift (Figure 5) shows that between redshifts $z = 1$ and $z = 2$ the ratio $\frac{K\text{-corr}_{175\ \mu\text{m}}}{K\text{-corr}_{90\ \mu\text{m}}}$ grows from 6 to 14: at $z = 2$ a similar galaxy has 14 times more flux at $175\ \mu\text{m}$ than at $90\ \mu\text{m}$.

The non-thermal emission is known to be strongly correlated with the FIR emission for starburst galaxies (e.g Helou et al. 1985), even if Sanders & Mirabel (1996) show an important scatter in the correlation. With ELAIS VLA identifications (42 sources), we compute $q = \log(F_{\nu\ \text{FIR}}) - \log(F_{\nu\ 1.4\ \text{GHz}})$ (we take $F_{175\ \mu\text{m}}$ for $F_{\nu\ \text{FIR}}$ and not a combination of $F_{60\ \mu\text{m}}$ and $F_{100\ \mu\text{m}}$) the FIR to 1.4 GHz log ratio. For 70 % of our sample $q < 2.3$, and $2.3 \leq q < 3$ for 30 %; the dispersion is significant and must be taken into account for deep radio observations.

7. CONCLUSION

We presented the FIRBACK $175\ \mu\text{m}$ survey, data reduction and analysis. Identifications of sources at various wavelengths, color ratios and source counts suggest that half of the sources are at redshifts greater than 1. Following-up these sources in order to have better positional accuracies, and SED constraints is now the key for understanding this population of dust enshrouded galaxies.

Additional information, images and papers are available online at <http://wwwfirback.ias.fr>

ACKNOWLEDGMENTS

We would like to thank M.A. Miville-Deschênes for his courtesy in permitting use of his image printing program, and C. Gabriel for fruitful discussions at ESA's ISO Data Centre (IDC) at Vilspa, Spain.

REFERENCES

- Becker, R.H., et al. 1995, ApJ, 450, 559
 Ciliegi, C. et al. 1998, astro-ph/9805353
 Condon, J.J., 1992, ARA&A, 30, 575
 Désert, F-X., et al. 1998 A&A, astro-ph/9809004
 Elbaz, D., et al. 1998, astro-ph/9807209
 Fixsen, D.J., et al. 1998, ApJ, 508, 123
 Franceschini, A., et al. 1998, MNRAS 296, 709
 Gabriel, C., et al. 1997, Proc. of the ADASS VI conf., ASP Conf. Ser., Vol.125, p108
 Gruppioni, C., et al. 1997, MNRAS, 286, 470
 Guiderdoni, B., et al., 1998, MNRAS 295, 877
 Hauser, M.G., et al. 1998 ApJ, 508, 25
 Helou, G., et al. 1985, ApJ, 298, L7
 Kawara, K., et al. 1998, A&A 336, L9
 Lagache, G., et al. 1999, A&A, in press, astro-ph/9901059
 Puget, J.L., et al. 1996, A&A 308, L5
 Puget, J.L., et al. 1999, A&A, in press, astro-ph/9812039
 Sanders, D.B., Mirabel, I.F., 1996, ARA&A 34, 749
 Stickel M., et al. 1998, A&A, 336, 116